Atmos. Chem. Phys., 14, 3623–3635, 2014
www.atmos-chem-phys.net/14/3623/2014/
doi:10.5194/acp-14-3623-2014

Atmospheric Chemistry and Physics
Open Access

Regional modeling of tropospheric NO_2 vertical column density over East Asia during the period 2000–2010: comparison with multisatellite observations

S. Itahashi[1,*], **I. Uno**[2], **H. Irie**[3], **J.-I. Kurokawa**[4], **and T. Ohara**[5]

[1]Department of Earth System Science and Technology, Kyushu University 6-1 Kasuga Park, Kasuga, Fukuoka, 816-8580, Japan
[2]Research Institute for Applied Mechanics, Kyushu University 6-1 Kasuga Park, Kasuga, Fukuoka, 816-8580, Japan
[3]Center for Environmental Remote Sensing, Chiba University 1-33 Yayoicho, Inage-ku, Chiba, 263-8522, Japan
[4]Asia Center for Air Pollution Research 1182 Sowa, Nishi-Ku, Niigata, 950-2144, Japan
[5]National Institute for Environmental Studies 16-2 Onogawa, Tsukuba, Ibaraki, 305-8506, Japan
[*]now at: Environmental Science Research Laboratory, Central Research Institute of Electric Power Industry 1646 Abiko, Abiko, Chiba, 270-1194, Japan

Correspondence to: S. Itahashi (syuichi@riam.kyushu-u.ac.jp, isyuichi@criepi.denken.or.jp)

Received: 21 March 2013 – Published in Atmos. Chem. Phys. Discuss.: 25 April 2013
Revised: 28 January 2014 – Accepted: 26 February 2014 – Published: 9 April 2014

Abstract. Satellite observations of the tropospheric NO_2 vertical column density (VCD) are closely correlated to, and thus can be used to estimate, surface NO_x emissions. In this study, the NO_2 VCD simulated by a regional chemical transport model with emissions data from the updated Regional Emission inventory in ASia (REAS) version 2.1 were validated through comparison with multisatellite observations during the period 2000–2010. Rapid growth in NO_2 VCD ($\sim 11\,\%\,\mathrm{year}^{-1}$) driven by the expansion of anthropogenic NO_x emissions was identified above the central eastern China (CEC) region, except for the period during the economic downturn. In contrast, slightly decreasing trends ($\sim 2\,\%\,\mathrm{year}^{-1}$) were identified above Japan accompanied by a decline in anthropogenic emissions. To systematically compare the modeled NO_2 VCD, we estimated sampling bias and the effect of applying the averaging kernel information, with particular focus on the SCanning Imaging Absorption spectroMeter for Atmospheric CHartographY (SCIAMACHY) data. Using the updated REAS, the modeled NO_2 VCD reasonably reproduced annual trends observed by multisatellites, suggesting that the rate of increase of NO_x emissions estimated by the updated REAS inventory would be robust. Province-scale revision of emissions above CEC is needed to further refine emission inventories. Based on the close linear relationship between modeled and observed NO_2 VCD and anthropogenic NO_x emissions, NO_x emissions in 2009 and 2010, which were not covered by the updated REAS inventory, were estimated. NO_x emissions from anthropogenic sources in China in 2009 and 2010 were determined to be 26.4 and $28.5\,\mathrm{Tg\,year}^{-1}$, respectively, indicating that NO_x emissions increased more than twofold between 2000 and 2010. This increase reflected the strong growth of anthropogenic emissions in China following the rapid recovery from the economic downturn from late 2008 until mid-2009. Our method consists of simple estimations from satellite observations and provides results that are consistent with the most recent inventory of emissions data for China.

1 Introduction

Nitrogen oxides ($NO_x = NO + NO_2$) emitted from anthropogenic sources (e.g., fossil fuel combustion) and natural sources (e.g., microbiological processes in soil) play key roles in tropospheric chemistry, with important implications for air quality and climate change. In particular, NO_x contributes to the formation of photochemical ozone (O_3) and secondary aerosols. It is also involved in the chemical

Published by Copernicus Publications on behalf of the European Geosciences Union.

formation of other atmospheric species through interaction with hydroxyl radicals (OH) (Seinfeld and Pandis, 2006).

In recent years, advances in satellite technology and the development of new instruments and algorithms have allowed for observations of the NO_2 vertical column density (VCD) from space, providing useful information for air-quality research (e.g., Richter et al., 2005; van der A et al., 2008; Irie et al., 2009). A global picture of the spatial distribution of the NO_2 VCD is now available because satellite measurements provide global coverage in a very short time (between 1 and 6 days depending on the instrument although more time is needed when cloud cover is present). Operational observations of tropospheric NO_2 VCD have been performed continuously for more than 10 years by the Global Ozone Monitoring Experiment (GOME), the SCanning Imaging Absorption spectroMeter for Atmospheric CHartographY (SCIAMACHY), the Ozone Monitoring Instrument (OMI), and the GOME-2. Because of the short lifetime of NO_x in the troposphere, satellite NO_2 observations are closely correlated to surface NO_x emissions. The tropospheric NO_2 VCD retrieved from satellites has been successfully used to evaluate and quantify the spatial distribution and long-term trends of NO_x emissions (He et al., 2007; Uno et al., 2007; van der A et al., 2008; Han et al., 2009; Lamsal et al., 2011; Schneider and van der A, 2012).

A large positive trend of NO_2 VCD over eastern China in parallel with a strong increase in NO_x emissions from 1996 to 2005 due to increases in industry and traffic has been identified using a combination of GOME and SCIAMACHY observations. The emissions rate accelerated during this period, from 4 % $year^{-1}$ in 1997 to 12 % $year^{-1}$ in 2002 (Richter et al., 2005). However, a systematic analysis of NO_2 VCD measured by GOME and simulated by a regional chemical transport model with anthropogenic emissions data from the Regional Emission inventory in ASia (REAS) version 1.1 (Ohara et al., 2007) revealed that a bottom-up emission inventory underestimates the rapid growth in NO_x emissions from China, especially from 1998 to 2000 (Uno et al., 2007). Emissions estimated using bottom-up methods involve large uncertainty because of the uncertainty in activity data such as energy consumption, removal efficiencies, emissions factors, and other variables. A combination of top-down and bottom-up methods provides one potential alternative approach (e.g., Martin et al., 2003). By developing a data assimilation system, NO_x emissions in an a priori REAS emission inventory were optimized to catch up with the rapid growth of emissions from China. The increase in NO_x emissions from 1996 to 2002 over eastern China was much larger for a posteriori than for a priori estimates (49 % vs. 19 %) (Kurokawa et al., 2009).

REAS inventory version 1.1 (Ohara et al., 2007) provides emissions data from 1980 to 2003 that have been utilized in many investigations; however, its coverage must be updated to reflect the recent status of emissions. Recently, the REAS emission inventories were updated to version 2.1 based on the same methodology as used in previous versions, but with updated activity data and parameters. The new data set covers the period from 2000 to 2008 with expanded target areas, including Russia and central Asia. The data set contains monthly variations in the individual sources and source categories with a $0.25^\circ \times 0.25^\circ$ grid resolution (Kurokawa et al., 2013). Emissions data are necessary inputs for chemical transport models, and evaluations of the new emission inventories are needed to improve knowledge about air quality over East Asia.

In this study, tropospheric NO_2 VCD over East Asia was simulated using a regional chemical transport model with the updated REAS inventory version 2.1, and observations by four satellites (GOME, SCIAMACHY, GOME-2, and OMI) were combined and analyzed. Long-term simulations between 2000 and 2010 with relatively high resolution (80 km) were made using a regional-scale, full-chemistry model, the most valuable aspect of this study. Previous studies of emission trends and their variability were conducted with relatively coarse resolution (e.g., Lin and McElroy, 2011; Lamsal et al., 2011). The fine-scale resolution used in the present study will enable comparison among emission inventories. We also focused on validating the newly updated REAS inventory. Decade-long trends in tropospheric NO_2 VCD over China, Korea, and Japan were examined, with an emphasis on corresponding changes in anthropogenic NO_x emissions. By utilizing multisatellite observations, variations in tropospheric NO_2 VCD in the morning and afternoon were also investigated. Moreover, on the basis of the clear linear relationships between modeled and observed NO_2 VCD and anthropogenic NO_x emissions, simplified inverse estimations for 2009 and 2010, which were not covered by the updated REAS inventory, were also proposed and compared with the latest emission inventories in China. The inverse estimation approach provides necessary information about the recent status of emissions over East Asia.

2 Modeling setup and satellite observations

2.1 Model description

Three-dimensional numerical simulations over East Asia were conducted using the regional chemical transport model of the Community Multi-scale Air Quality (CMAQ) modeling system version 4.7.1 (Byun and Schere, 2006) released by the United States Environmental Protection Agency (EPA). CMAQ modeling systems have been used extensively for atmospheric environmental research over East Asia (e.g., He et al., 2007; Uno et al., 2007; Han et al., 2009; Itahashi et al., 2012a, 2012b, 2013). In this study, the meteorological fields were generated by the Weather Research and Forecasting (WRF) model version 3.3 with the National Centers for Environmental Prediction (NCEP)/National Center for Atmospheric Research (NCAR) reanalysis data (FNL;

http://rda.ucar.edu/datasets/ds083.2/). The model was constructed with a 98×78 horizontal grid at a resolution of 80 km, centered at 35° N, 115° E on a Lambert conformal projection, with 37 vertical grids extending from the surface to 50 hPa. Emissions data for the CMAQ model were prepared as follows. Anthropogenic emissions data were obtained from the newly updated REAS version 2.1 (Kurokawa et al., 2013). Natural sources of NO_x from soil were also obtained from the updated REAS. Monthly variation estimated by the updated REAS inventory was included in this study (Fig. 9 of Kurokawa et al., 2013), but diurnal variation was not considered. Emissions from biogenic and biomass burning, with monthly variations, were obtained from the Model of Emissions of Gases and Aerosols from Nature (MEGAN) (Guenther et al., 2006) and the Global Fire Emissions Database (GFED) version 3.1 (van der Werf et al., 2010), respectively. Lightning emissions were not considered in this study because of the difficulty of determining their magnitude and variability.

The CMAQ modeling system was configured as follows. A mass-conserving scheme ("yamo" scheme) was used for both horizontal and vertical advection (Odman and Russel, 2000). A single eddy diffusion algorithm ("multiscale" scheme) and a simple eddy-viscosity scheme ("eddy" scheme) were adopted for horizontal and vertical diffusion, respectively (Byun and Ching, 1999). The Statewide Air Pollution Research Center version 99 (SAPRC-99) chemical mechanism (Carter, 2000) and the fifth-generation CMAQ aerosol mechanism ("AERO5" scheme) (Carlton et al., 2010) were respectively adopted for production of gas-phase chemistry and aerosol chemistry. The initial conditions were provided in the CMAQ default data set, and lateral boundary conditions were generated using the results of the CHemical Atmospheric general circulation model for Study of atmospheric Environment and Radiative forcing (CHASER) global chemistry model (Sudo et al., 2002), with a monthly-mean basis. The model results were interpolated into $0.5° \times 0.5°$ resolution for analysis.

Numerical simulations using the updated REAS emission data were performed for the period 2000–2008 (see Table 5 in Kurokawa et al., 2013 for temporal variations in annual emissions), and emissions from anthropogenic sources were fixed for 2009 and 2010 using the same inventory as 2008 for a sensitivity simulation. Data on other sources of emissions (biogenic and biomass burning) from 2009 and 2010 were utilized with monthly variation in the sensitivity simulation.

2.2 Satellite observation data

GOME, SCIAMACHY, GOME-2, and OMI data were analyzed in this study. The specifications of these instruments are summarized in Table 1. The GOME, SCIAMACHY, and GOME-2 data were used for morning observations, and the OMI data were used for afternoon observations. The level-2 products of TM4NO2A version 2.0 were used. These were developed at the Royal Netherlands Meteorological Institute (KNMI) and are available from the Tropospheric Emission Monitoring Internet Service (TEMIS) at www.temis.nl. The retrieval process for tropospheric NO_2 VCD was as follows. (1) The NO_2 slant column density (SCD) was obtained from the reflectance spectra using the differential optical absorption spectroscopy (DOAS) technique. (2) The stratospheric and tropospheric contributions to the NO_2 SCD were separated by assimilating the NO_2 SCD into the TM4 chemistry-transport model. (3) The tropospheric air mass factor (AMF) was incorporated to convert the tropospheric NO_2 SCD into the tropospheric NO_2 VCD (e.g., Boersma et al., 2007). Improvements in the version 2.0 products compared to version 1.0 included an updated albedo database, improved AMF and surface-height calculations, and a new version of the TM4 chemistry-transport model (e.g., Boersma et al., 2011).

The observed NO_2 VCDs were analyzed from January 2000 to July 2003 for GOME, from August 2002 to December 2010 for SCIAMACHY, from January 2007 to December 2010 for GOME-2, and from October 2004 to December 2010 for OMI. The satellite observation data set providing the location and value for each measurement pixel was interpolated into $0.5° \times 0.5°$ resolution and only used during cloud-free conditions (cloud cover less than 20 %). Among the four satellite measurements, the spatial resolution of GOME is relatively larger than that of the other instruments, which would lead to measurement biases. Measurement from the other three satellites, SCIAMACHY, GOME-2, and OMI, did not exhibit significant bias compared to ground-based Multi-Axis Differential Optical Absorption Spectroscopy (MAX-DOAS) observations during daytime at Chinese sites (Irie et al., 2012). It should be noted that this evaluation was conducted in summer (mainly in June) under tight spatial coincidence criteria (tighter than 0.5° latitude and longitude). However, satellite biases during winter were not evaluated with ground-based MAX-DOAS; such evaluation would help to reduce the uncertainty in satellite retrievals.

Retrieved NO_2 VCD data from satellites contain large uncertainty in the tropospheric AMF due to cloud fraction, surface albedo, a priori-assumed NO_2 profile, and the presence of aerosols (Boersma et al., 2004). It is important to include averaging kernel (AK) information into model simulations to eliminate the effects of error in a priori vertical profiles (e.g., Lin and McElroy, 2011). Nevertheless, model simulations can provide full temporal coverage when satellite observations are not available. Therefore, to systematically compare model results and satellite retrievals, we prepared three model data sets: (a) simply selected model results at 10:00 local time (LT) and 14:00 LT as representative of morning and afternoon, (b) model results sampled with valid pixels from satellite observations, and (c) model results sampled with valid pixels and besides the AK information of satellite observations applied. We were primarily interested

Table 1. Summary of satellite-based NO_2 measurement instruments.

Instrument	GOME	SCIAMACHY	GOME-2	OMI
Satellite	ERS-2	ENVISAT	MetOp-A	Aura
Period	April 1995–June 2003	March 2002–April 2012	October 2006–	July 2004–
Overpass time	10:30 LT	10:00 LT	09:30 LT	13:45 LT
Nadir-view spatial resolution	40 km × 320 km	30 km × 60 km	40 km × 80 km	13 km × 24 km
Global coverage	3 days	6 days	1 day	1 day

in long-term trends, so we comprehensively analyzed model data sets (b) and (c) for the SCIAMACHY retrieval data. Because obtaining global coverage of SCIAMACHY data takes longer than other satellite data (Table 1), SCIAMACHY contains fewer valid data. Therefore, GOME-2 and OMI would involve less sampling bias.

3 Results and discussion

3.1 Tropospheric NO_2 column trends

Tropospheric NO_2 VCD above central eastern China (CEC; 110–123° E, 30–40° N), Korea (125–130° E, 34.5–39° N), and Japan (133–141° E, 33.5–37° N) were examined (see top-left panel in Fig. 3). In Fig. 1, the temporal variations in monthly mean tropospheric NO_2 VCD above CEC are shown for (a) morning and (b) afternoon. Both the model results and satellite observations clearly illustrated the rapid increase in NO_2 VCD above the CEC between 2000 and 2010, except during the economic downturn between late 2008 and mid-2009 (e.g., Lin and McElroy, 2011). The peak levels of monthly mean NO_2 VCD in the winter in 2009–2010 indicated a rapid recovery. CMAQ modeling results reproduced the observed temporal variation but greatly underestimated the high NO_2 VCD in the mornings during winter. However, they remarkably captured the absolute values throughout the year between 2000 and 2008 in the afternoon. In the model simulations, a sensitivity study during 2009–2010 with anthropogenic emission fixed at 2008 levels was conducted. The large differences between model and satellite observations also reflected the recovery of the Chinese economy and corresponding increases in emissions from 2009–2010 compared to 2008 levels. These differences were larger and clearer in the morning than in the afternoon because of the inhibition of NO_x-related chemistry under low photolysis rates and intense emissions during the morning rush hour.

To further investigate the effect of the economic downturn, in the lower part of Fig. 1, tropospheric NO_2 VCD was normalized to averaged values between October 2007 and September 2008 with a 12 month moving window, and analyzed according to the method described by Lin and McElroy (2011). Model results obtained using the updated REAS inventory reproduced the growth rate of NO_2 VCD remarkably well in the morning (Fig. 1a) and afternoon (Fig. 1b),

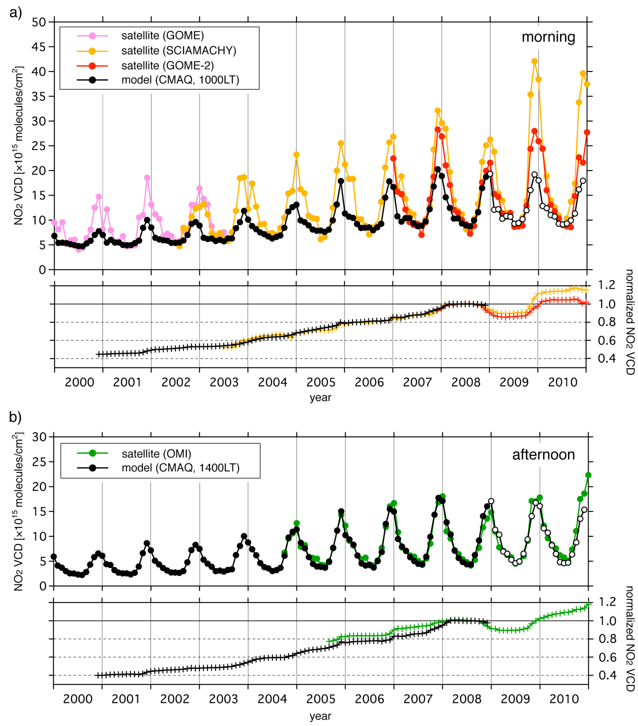

Fig. 1. Temporal variations in monthly mean tropospheric NO_2 VCD above the central eastern China (CEC) region during the period 2000–2010 from multisatellite observations (GOME, SCIAMACHY, GOME-2 and OMI) and model results (open circles denote sensitivity simulations with anthropogenic emissions fixed at 2008 values) in the **(a)** morning and **(b)** afternoon. The normalized tropospheric NO_2 VCD relative to averaged values between October 2007 and September 2008 with a 12 month moving average are also shown at the bottom.

and suggested that the NO_2 VCD approximately doubled between 2001–2002 and 2008 (before the economic downturn).

Model reproducibility was systematically compared with the data sets obtained by sampling the valid pixels of the SCIAMACHY data and by applying the AK information in the SCIAMACHY data. Figure 2 presents monthly variations of NO_2 VCD above CEC in 2005. The sample bias was relatively small: model results simply selected at 10:00 LT and those sampled with valid SCIAMACHY data agreed to within 10 %. This good agreement could be partly attributed to the relatively larger area analyzed. However, application of

AK information to the model results dramatically increased the modeled NO_2 VCD during winter, by up to 33.4 % in November 2005. The effect of AK was relatively small in summer (∼ 10 % difference).

The seasonal variation in tropospheric NO_2 VCD above CEC is shown as summer minima and winter maxima (Figs. 1, 2). Modeled results underestimated in the morning during winter above CEC (Fig. 1a), even when AK was applied to the model results (Fig. 2). Comparisons between the spatial distribution of modeled and retrieved tropospheric NO_2 VCD in the morning are presented in Fig. 3 (model results selected at 10:00 LT) and Fig. 4 (model results sampled and the AK of the SCIAMACHY data applied), with a focus on the summer (June–August 2005) and winter (December 2005–February 2006). In summer, due to the short lifetime of NO_x, the highest NO_2 VCDs were found around megacities such as Beijing, Shanghai, Hong Kong, Seoul, and Tokyo and in the North China Plain region. The model reproduced the spatially averaged temporal variation in NO_2 VCD over the CEC region (Fig. 1a) but overestimated it in Hebei and Henan Provinces and underestimated it in Shanxi Province (Fig. 3). These features also appeared when the AK information was applied to the model results (Fig. 4). The general agreement between model results with and without application of AK information indicated relatively lower uncertainty of the a priori profile in the satellite retrieval and consistency between the CMAQ and TM4 chemical transport models during summer. The SCIAMACHY overpass time would be at the diurnal minimum of lightning activity, but consideration of lightning emissions would help improve the underestimation of model results because many lightning strikes occur in summer (e.g., Lin, 2012). In winter, high NO_2 VCD covered the entire CEC region, and the model generally underestimated values in this region. The model results with AK applied also suggested model reproducibility was underestimated, but the differences were smaller (especially above the CEC region) and model overestimation was found in Hebei Province. These findings suggest large uncertainty in a priori profile shapes and a lack of consistency between the CMAQ and TM4 models during winter.

Problems in both modeling and retrieval may have contributed to the discrepancies in NO_2 VCD above CEC during winter. Emission intensity is considered to be one of the most significant factors in the model simulations. When uncertainty in the a priori profile was eliminated by applying the AK information to the model results, differences between modeled and retrieved NO_2 VCD generally displayed the same spatial pattern as that seen in summer (Fig. 4). In the updated REAS inventory, activity data are based on the province-level energy tables; hence, revision of emissions at the province-level scale may be required to further improve accuracy. Here, we note that the uncertainty of total anthropogenic emissions from China in the updated REAS was relatively lower in 2005 compared to other emission inventories (Fig. 7). Modeling uncertainties in meteorology and chemistry are also important factors. Modeled cloud optical depth, the uptake coefficient of the hydroperoxyl radicals (HO_2) by aerosols, and some rate constants have been found to have a large impact on NO_2 VCD in the GEOS-Chem global chemistry model (Lin et al., 2012), and these issues would be also relevant to the CMAQ regional chemistry model. Their approach would offer a comprehensive understanding based on current knowledge and should be applied in a regional-scale chemical transport model. For satellite observations, with the exception of uncertainty in the a priori vertical profiles, it may be difficult to retrieve wintertime NO_2 VCD values of the same quality as summertime values because of the more stable, shallow boundary-layer conditions in winter. As indicated in Fig. 1, large differences in retrieved NO_2 VCD among SCIAMACHY and GOME-2 satellite observations were observed in winter, so validation of satellite measurements by comparing them with ground-based observations (e.g., MAX-DOAS) during winter is required to clarify this uncertainty.

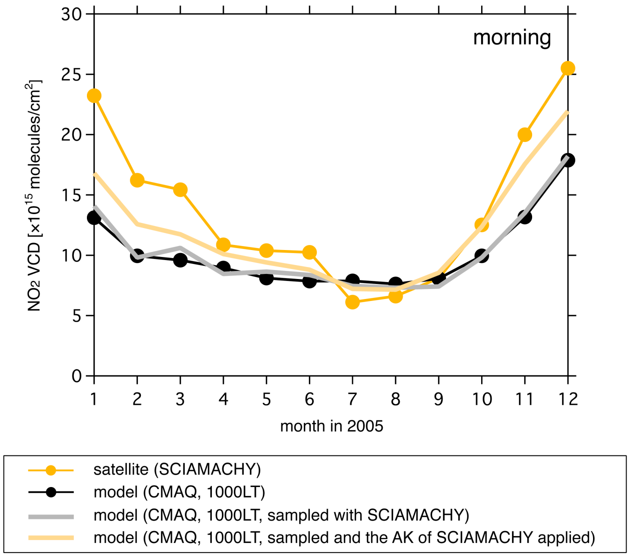

Fig. 2. Modeling reproducibility of monthly mean tropospheric NO_2 VCD above central eastern China (CEC) in 2005. Model results are shown for three data sets: simply selected at 10:00 LT (black line), sampled with valid pixels of the SCIAMACHY data (gray line), and sampled with valid pixels and besides the averaging kernel (AK) information of the SCIAMACHY data applied (light-orange line).

Figure 5 illustrates annual mean tropospheric NO_2 VCDs over CEC, Korea, and Japan (rectangular region in Fig. 3) during the period 2000–2010, along with the temporal variation in total anthropogenic NO_x emissions from China, Korea, and Japan estimated using the updated REAS inventory; model results simply selected at 10:00 and 14:00 LT are presented. Table 2 lists sampling biases and the effect of application of AK with the SCIAMACHY data. The model tended to underestimate the tropospheric NO_2 VCD in the

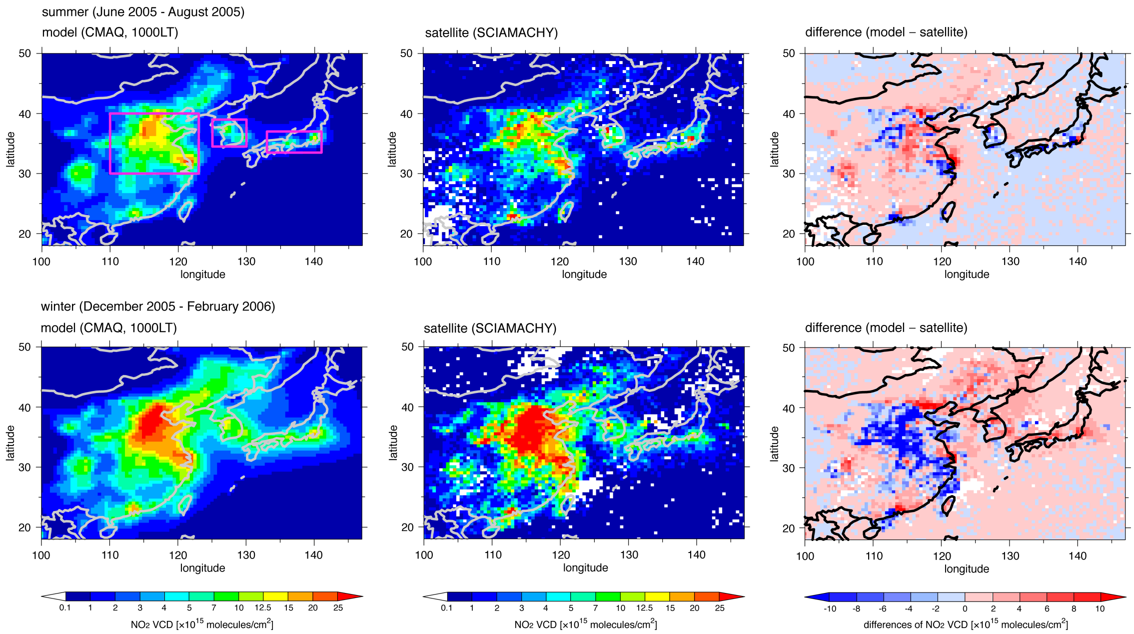

Fig. 3. Spatial distribution of tropospheric NO_2 VCD from (left) model results at 10:00 LT, (center) satellite observations by SCIAMACHY, and (right) the differences between model and satellite in (top) summer (averaged between June 2005 and August 2005) and (bottom) winter (averaged between December 2005 and February 2006). The rectangular regions shown in the top-left figure are the investigated regions (central eastern China (CEC), Korea, and Japan).

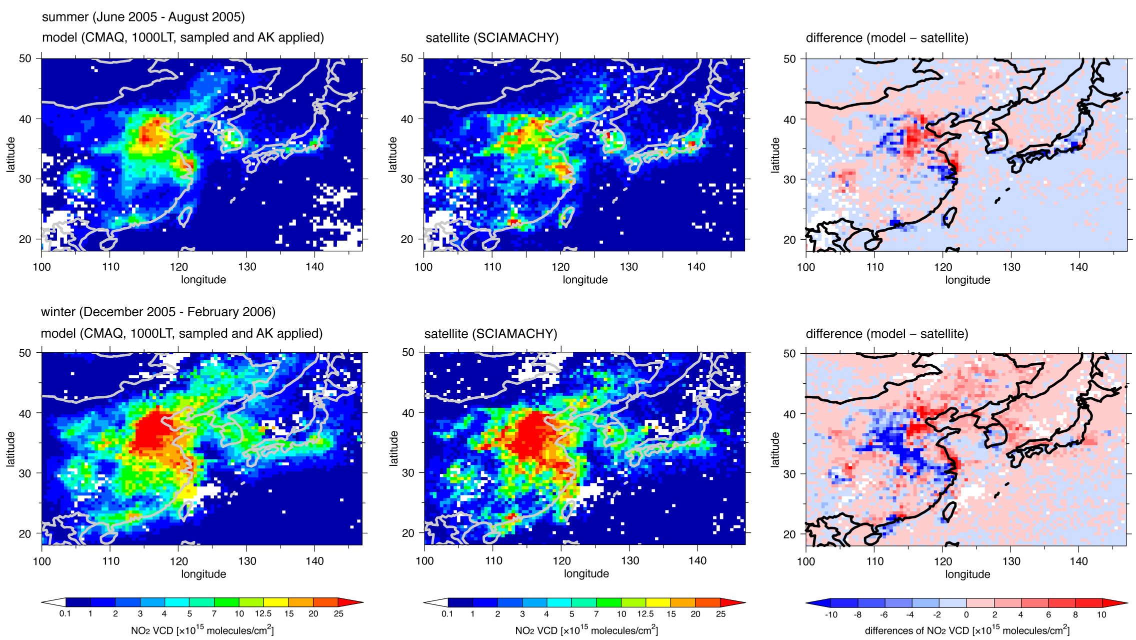

Fig. 4. Same as Fig. 3, but model results are sampled with valid pixels and the averaging kernel (AK) information of SCIAMACHY data applied.

Table 2. Modeling reproducibility of annual mean NO_2 VCD compared to SCIAMACHY data.

	Modeled NO_2 VCD ($\times 10^{15}$ molecules cm^{-3})			Relative change in modeled NO_2 VCD from (a) (%)		Statistical comparison of modeling reproducibility with satellite data					
						Normalized mean bias (%)			Normalized mean error (%)		
Year	(a)[a]	(b)[b]	(c)[c]	(b)	(c)	(a)	(b)	(c)	(a)	(b)	(c)
central eastern China (CEC)											
2003	7.3	7.3	8.4	0.9	15.4	−31.0	−30.4	−20.4	31.9	31.6	20.4
2004	8.4	8.2	10.0	−2.9	18.3	−23.7	−25.9	−9.7	23.7	25.9	10.6
2005	10.2	10.3	12.0	1.3	18.1	−26.0	−25.1	−12.7	29.4	27.6	15.2
2006	10.4	10.3	12.1	−0.8	15.9	−27.2	−27.7	−15.6	28.8	28.1	16.0
2007	12.0	11.6	13.8	−3.3	15.1	−26.0	−28.4	−14.8	27.9	30.2	17.0
2008	12.5	12.6	15.5	0.2	24.0	−25.1	−25.0	−7.2	26.9	26.3	11.1
Korea											
2003	5.7	6.1	5.7	7.2	−0.6	−13.5	−7.3	−14.0	27.8	23.9	21.6
2004	5.6	5.6	5.9	0.1	4.9	−18.1	−18.0	−14.2	21.2	19.3	16.4
2005	5.5	5.6	5.6	1.4	1.7	−14.7	−13.5	−13.2	28.9	30.1	25.6
2006	5.5	5.4	5.6	−2.9	2.1	−15.8	−18.2	−14.0	18.4	19.9	17.9
2007	5.4	5.1	5.4	−5.1	−0.8	−19.7	−23.8	−20.3	26.6	28.6	26.8
2008	5.1	5.0	5.3	−1.3	4.8	−28.4	−29.4	−25.0	33.9	32.2	27.5
Japan											
2003	4.8	4.9	4.0	3.2	−16.1	−11.8	−8.9	−25.9	18.7	21.1	26.0
2004	4.5	4.7	4.2	3.1	−6.3	−29.7	−27.5	−34.1	30.1	29.2	34.1
2005	4.6	4.8	4.3	3.3	−6.8	−26.9	−24.5	−31.9	28.8	30.0	32.6
2006	4.4	4.7	3.9	4.9	−11.9	−14.0	−9.8	−24.3	21.5	20.0	24.8
2007	4.4	4.3	4.0	−0.6	−8.7	−28.5	−28.9	−34.7	28.5	28.9	34.7
2008	4.0	4.2	3.9	5.5	−2.8	−23.5	−19.4	−25.7	27.9	27.6	29.0

[a] Model results are simply selected at 10:00 LT. [b] Model results are sampled with valid pixels of SCIAMACHY data. [c] Model results are sampled with valid pixels and the averaging kernel (AK) information of SCIAMACHY data applied.

morning during winter over CEC (Fig. 5a), hence the annual mean NO_2 VCD was also underestimated. Because of the increase of NO_2 VCD during winter obtained by applying the AK to model results (Fig. 2), modeled mean annual NO_2 VCD was changed by +15.0 % from the model results simply selected at 10:00 LT (Table 2). The statistical analyses of normalized mean bias (NMB) and normalized mean error (NME) between model results and the SCIAMACHY data were improved by more than 10 % by applying the AK (Table 2). The growth rates of tropospheric NO_2 VCD from 2003–2008 were +11.4 % $year^{-1}$ (model, 10:00 LT), +11.5 % $year^{-1}$ (model, 10:00 LT, sampled and with AK applied) and +11.8 % $year^{-1}$ (satellite, SCIAMACHY). During the same period, the updated REAS estimated +9.1 % $year^{-1}$ growth in NO_x emissions from anthropogenic sources. In the afternoon, the tropospheric NO_2 VCD also exhibited growth of +11.6 % $year^{-1}$ (CMAQ, 14:00 LT) and +8.9 % $year^{-1}$ (satellite, OMI) between 2005 and 2008. The differences between satellite observations and models with sensitivity simulations in 2009 and 2010 (open circles in Fig. 5) again showed a growth in emissions during 2009–2010 after the recovery from the economic downturn. Above Korea (Fig. 5b), both satellite observations and model results showed complex variability. The tropospheric NO_2 VCD showed an initial peak during 2003–2004 and then a decrease toward 2006. Following this, the satellite observations exhibited an increasing trend from 2007 by SCIAMACHY and a flat trend by GOME-2. The model indicated a slightly decreasing trend for 2007–2008 due to the reduction in anthropogenic NO_x emissions. Sampling bias and the effect of AK was approximately ±5 % for modeling reproducibility, and NMB and NME results were improved by ∼ 5 % (Table 2). In the afternoon, the tropospheric NO_2 VCD was constant above Korea. In Japan (Fig. 5c), slightly decreasing trends of tropospheric NO_2 VCD between 2000 and 2010 were revealed, along with a decline in emissions in both morning and afternoon. Above Japan, in contrast to the CEC region and Korea, application of the AK led to a reduction in modeled NO_2 VCD. Compared to the SCIAMACHY observations, modeled NO_2 VCD above Japan was worsened

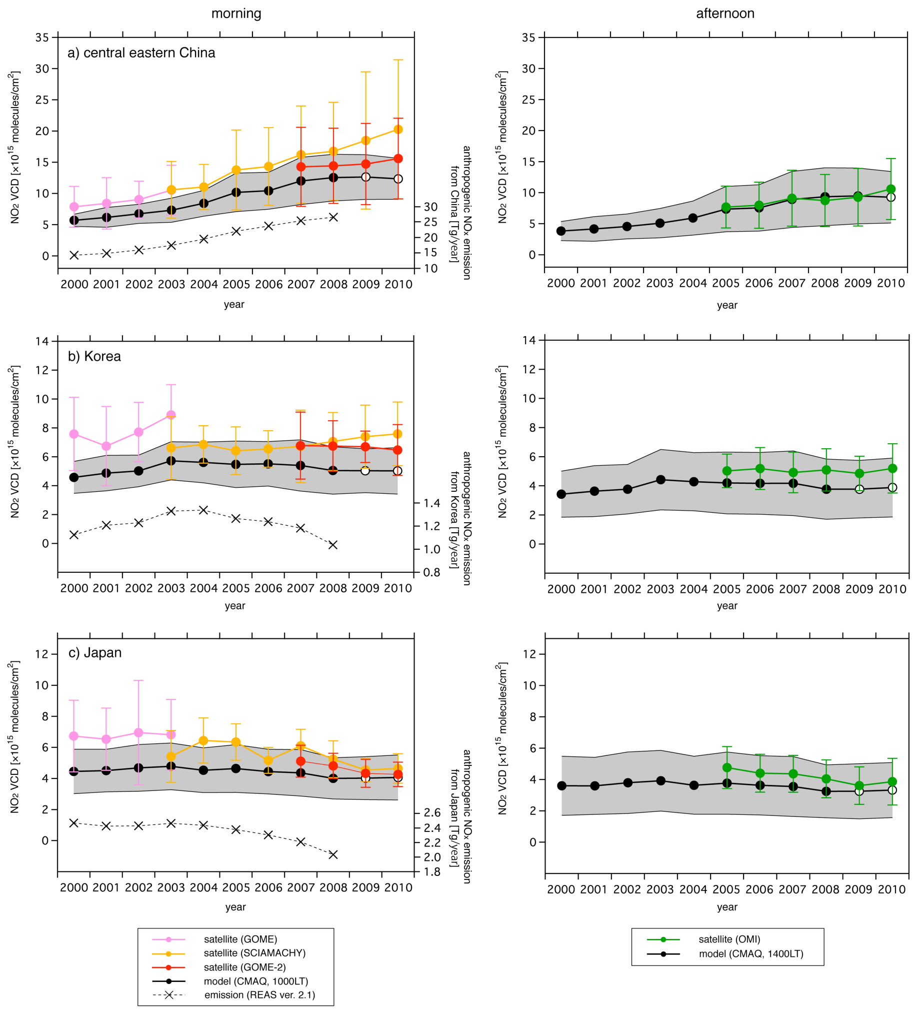

Fig. 5. Trend in annual mean tropospheric NO_2 VCD during the period 2000–2010 from multisatellite observations (GOME, SCIAMACHY, GOME-2, and OMI) and model results (open circles denote sensitivity simulations with anthropogenic emissions fixed at 2008 values) above **(a)** central eastern China (CEC), **(b)** Korea, and **(c)** Japan, in the (left) morning and (right) afternoon. Bars and shaded areas indicate one standard deviation.

by 5–15 % for NMB and NME (Table 2). In the morning, the tropospheric NO_2 VCD during 2003–2008 declined by $-2.3\,\%\,\mathrm{year}^{-1}$ (model, 10:00 LT), $-1.8\,\%\,\mathrm{year}^{-1}$ (model, 10:00 LT, sampled and with AK applied), and $-1.5\,\%\,\mathrm{year}^{-1}$ (satellite, SCIAMACHY), and the updated REAS estimated a $3.6\,\%\,\mathrm{year}^{-1}$ reduction of NO_x emissions in Japan during the same period. In the afternoon, the tropospheric NO_2 VCD also exhibited declines of $-4.6\,\%\,\mathrm{year}^{-1}$ (CMAQ, 14:00 LT) and $-4.6\,\%\,\mathrm{year}^{-1}$ (satellite, OMI) between 2005 and 2008. Above Korea and Japan, fewer data could be used to calculate the spatial averaging compared to CEC, and GOME observation data appeared to be biased in part because of the relatively coarse resolution (Table 1). The modeled results simply selected at the local overpass time of satellite observations captured well the observed long-term trends obtained by satellite measurements, and application of the AK information to the model results further improved the reproducibility. To summarize, for the annual trend in NO_2 VCD, model simulations utilizing the updated REAS emission inventory version 2.1 reproduced the tropospheric NO_2 VCD observed by multisatellites reasonably well.

It should be noted that the absolute values of modeled NO_2 VCD displayed improved accuracy compared to those in our previous study (He et al., 2007; Uno et al., 2007). Modeled NO_2 VCD were reported to be lower than observed values by factors of 2–4 over polluted CEC; however, our modeling system reproduced NO_2 VCD well except for mornings in wintertime, and quantitative discussion of NO_2 VCD is possible in this study. Changes in the modeling system were made in (1) the vertical resolution; (2) updating of the CMAQ modeling system itself, including the chemical reaction scheme; and (3) use of the updated REAS emission inventory. Changes in NO_2 VCD due to the numbers of vertical layers were negligible according to the results of sensitivity simulations (Irie et al., 2013). To investigate the effect of NO_x emissions intensity on modeled NO_2 VCD, we compared the model results using the previous REAS inventory (Ohara et al., 2007). Modeling with the updated REAS produced a 13 % larger NO_2 VCD above the CEC region, along with a 9 % increase in anthropogenic NO_x emissions during 2003 (see Kurokawa et al., 2013, Table 5). It has been reported that the previous REAS inventory underestimated anthropogenic emissions over China (Kurokawa et al., 2009); using the updated REAS data, the model reproducibility was more reliable compared to satellite measurements of NO_2 VCD. Taken together, the most likely explanation for the improvements in quantitative reproducibility would be a change in the chemical reaction schemes, which control the lifetime of NO_2. Specifying these chemical reactions is beyond the scope of this study, but investigation of the uncertainties in chemical processes would provide valuable insight into the modeling reproducibility of NO_2 VCD, as suggested in recent studies (Lin et al., 2012; Stavrakou et al., 2013).

To clarify the discrepancies between satellite observations and model results found over Korea after 2007, and to validate the model results with updated REAS data, a comparison with other emission inventories would be useful. After applying the AK of the SCIAMACHY data into the model results, modeled NO_2 VCD after 2007 exhibited a slightly increasing trend that was consistent with SCIAMACHY but inconsistent with emission trends. Three inventories (including the previous REAS inventory) covering South Korea have revealed large discrepancies in high-emission metropolitan areas such as Seoul, Incheon, and Busan (Han et al., 2009). As noted above (Figs. 3, 4), province- and smaller-scale revisions of inventories based on a fine-resolution, full-chemistry model are necessary to establish more reliable emission inventories for Asia.

3.2 Inverse estimation of anthropogenic NO_x emissions

The NO_2 VCD modeled with the updated REAS emission inventory version 2.1 generally captured the temporal variation in the observed NO_2 VCD from multisatellite observations and corresponded with the fluctuations in NO_x emissions from anthropogenic sources above China, Korea, and Japan. A simple inverse estimation of annual NO_x emissions using tropospheric NO_2 VCD observations is proposed, focusing on the CEC region. The relationships among modeled and observed NO_2 VCD and anthropogenic NO_x emissions above CEC estimated by the updated REAS inventory are presented in Fig. 6. In this comparison, only the SCIAMACHY data were used because that data set for the morning was considered to have a more direct relationship with emissions and SCIAMACHY has longer archives than the other satellites. The coverage of SCIAMACHY data is less than that of the other satellites; however, potential uncertainties associated with the combination of different data sets with differences in spatial resolution, sensor calibration, local overpass time, and retrieval algorithms could be avoided by using only the SCIAMACHY data (e.g., Schneider and van der A, 2012). Because of the underestimation in modeled NO_2 VCD in winter, the slope of the linear regression results was larger than unity, but a close linear relationship could be seen (Fig. 6a). Furthermore, the relationships between the modeled NO_2 VCD and anthropogenic NO_x emissions from CEC were also clearly linear (Fig. 6b). When the model results adopted the AK information with SCIAMACHY data, clear linear regression was found, with a slope of almost unity and little degradation of the correlation coefficient. The modeled NO_2 VCD was calculated using various emission sources (e.g., anthropogenic, biomass burning, and biogenic emissions), but was mainly attributable to anthropogenic sources (Itahashi et al., 2013).

Hereafter, a simple estimate of NO_x emissions from the CEC region is introduced. On the basis of the close linear relationship between observed and modeled NO_2 VCD during the period 2003–2008, the modeled NO_2 VCD in 2009 and 2010 could be estimated from the linear regression results in Fig. 6a. After the modeled NO_2 VCD in 2009 and 2010 were estimated from the regression results, the anthropogenic emissions from CEC were assessed based on the close linear relationship in Fig. 6b. The results showed that the estimated anthropogenic NO_x emissions from CEC in 2009 and 2010 were 13.7 and 14.9 Tg year^{-1}, respectively. The CEC emissions made up approximately 46 % (44.4–47.2 % between 2000 and 2008 on an annual basis) of the emissions from China as a whole. Using this ratio in the updated REAS inventory, anthropogenic NO_x emissions from China in 2009 and 2010 were estimated at 27.2 (26.8–27.5) and 29.6 (29.1–29.9) Tg year^{-1}, respectively. Using the model with the AK applied yielded results of 26.4 (26.1–26.8) and 28.5 (28.1–28.9) Tg year^{-1} for China in 2009 and 2010, respectively. Note that this estimation would change as a result of different growth rates between the CEC region and other regions in China. Furthermore, considering that the anthropogenic NO_x emissions from China were estimated as 12.7 Tg year^{-1} in 2000 in the updated REAS emission inventory (Kurokawa et al., 2013), anthropogenic NO_x emissions from China beyond doubled between 2000 and 2010. The observed tropospheric NO_2 VCD declined during the economic recession between late 2008 and mid-2009, but the rapid recovery in winter of 2009–2010 led to a clear increase in anthropogenic NO_x emissions. It should be noted that when we used the observed NO_2 VCD measured by OMI from linear regression results, the estimated anthropogenic NO_x emissions from CEC in 2009 and 2010 were 12.6 and 14.3 Tg year^{-1}, respectively, which are consistent with the results obtained from SCIAMACHY data.

Our results indicated 6.8 % year^{-1} growth from model results simply selected at 10:00 LT, and 6.0 % year^{-1} growth from model results sampled and with the AK of the SCIAMACHY data applied. These are consistent with the findings of Lamsal et al. (2011), who estimated an annual

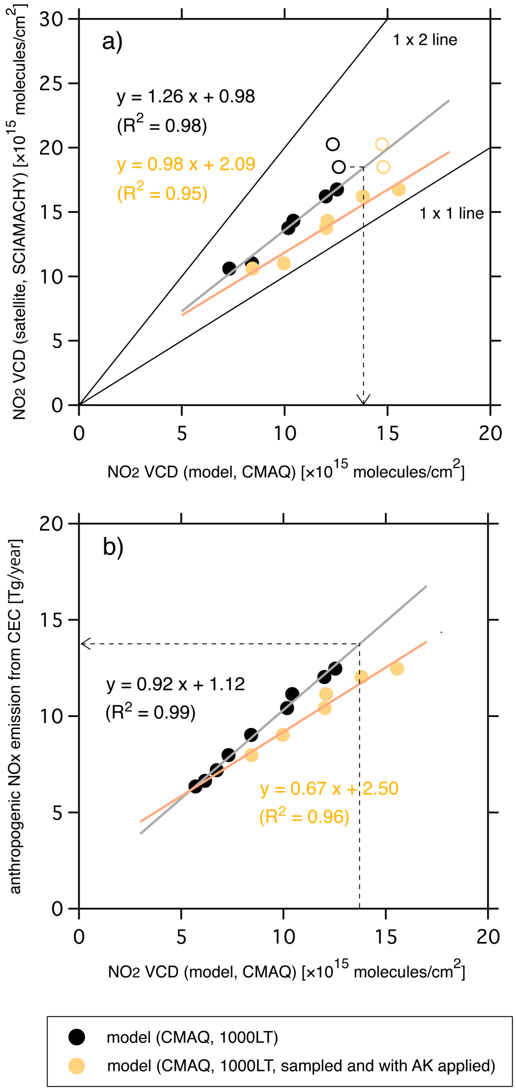

Fig. 6. Scatter diagrams of **(a)** annual-mean modeled and observed (SCIAMACHY) tropospheric NO_2 VCD above central eastern China (CEC). Open circles denote sensitivity simulations with anthropogenic emissions fixed at 2008 values. **(b)** Annual-mean modeled tropospheric NO_2 VCD above CEC with annually-based anthropogenic NO_x emissions from CEC. Symbol colors denote model results at 10:00 LT (black circles), and model results sampled with valid pixels and the averaging kernel (AK) information of SCIAMACHY data applied (light-orange circles).

growth rate of 6.7 % in China during the same period based on their β method using model-based sensitivity and satellite observation data. Figure 7 provides a summary of the comparison between the latest estimations of NO_x emissions in China, which covered the period 2005–2010 (He et al., 2012; B. Zhao et al., 2013; and Y. Zhao et al., 2013) and our estimated results. In this work, the inverse estimation without incorporating AK led to the overprediction of emissions. Our methodology, based on a close linear relationship, provides

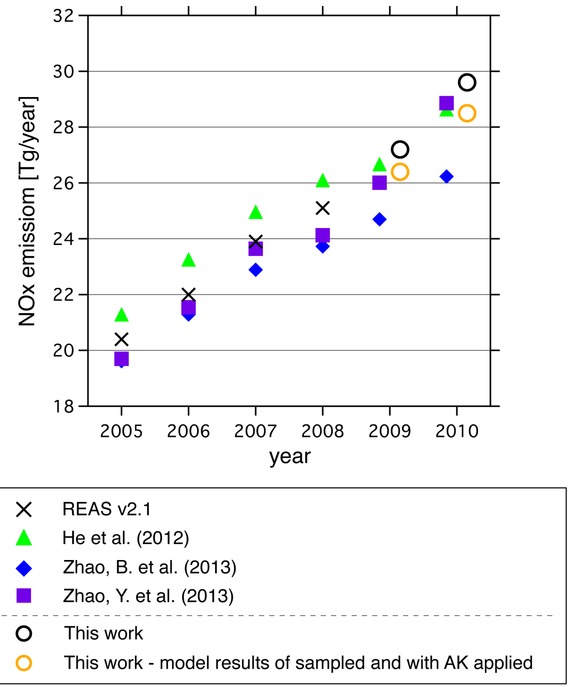

Fig. 7. Comparison of estimated NO_x emissions from China in this work and in other studies.

a simple way to estimate emissions, providing results that are relatively consistent with state-of-the-art emission estimations research. This kind of simple estimate provides valuable information for examining rapid changes in emissions resulting from economic shifts and/or control measures.

In our previous study, anthropogenic SO_2 emissions from China were inversely estimated based on the observed SO_2 column density above China and aerosol optical thickness in the downwind region. We determined that anthropogenic SO_2 emissions from China in 2009 were equivalent to those in 2004 (Itahashi et al., 2012a, 2012b). The reduction in SO_2 emissions after 2006 was a result of the widespread installation of flue-gas desulfurization under the eleventh Five-Year Plan (2006–2010) (Lu et al., 2010). As we have determined in this study, anthropogenic NO_x emissions exhibited a strong positive increase during 2000–2010. In contrast, the regulations imposed by the twelfth Five-Year Plan (2011–2015) of the Chinese government aimed to reduce NO_x emissions. Combining numerical simulations with satellite observations would enable an assessment of the changes in air quality over East Asia and serve as a more efficient method of updating emission inventories to keep pace with the rapid changes in anthropogenic emissions resulting from variations in economic activity and advances in pollution-control measures.

4 Conclusions

This study investigated tropospheric NO_2 VCD over East Asia from 2000 to 2010 based on a combined analysis of CMAQ model simulations with an updated REAS emission inventory and multisatellite observations (GOME, SCIAMACHY, GOME-2, and OMI). Rapid growth ($\sim 11\,\%\,\mathrm{year}^{-1}$) in tropospheric NO_2 VCD along with expanding anthropogenic emissions was identified above the CEC region in both model results and satellite observations. During the economic recession between late 2008 and mid-2009 (e.g., Lin and McElroy, 2011), the peak levels of NO_2 VCD in winter 2008–2009 were significantly lower than those in winter 2007–2008. However, satellite observations indicated a rapid recovery during winter 2009–2010. The model simulations closely reproduced the growth rate of NO_2 VCD in both the morning and afternoon and showed an approximate doubling of tropospheric NO_2 VCD from 2001–2002 to 2008 (before the economic downturn). In contrast to the results for the CEC region, the NO_2 VCD over Japan displayed a slight decreasing trend ($\sim 2\,\%\,\mathrm{year}^{-1}$), with a continuous reduction in anthropogenic emissions. Above Korea, the NO_2 VCD increased toward 2003–2004 before decreasing by 2006. Model results and satellite observations differed in the morning, but both revealed a constant trend of NO_2 VCD above Korea in the afternoon. Modeled NO_2 VCD was systematically compared by considering the sampling bias and the effect of application of AK information with retrieval data. Above CEC, AK had a relatively small effect in summer; but the model results agreed better with observed NO_2 VCD in winter by eliminating uncertainty in the a priori retrieval profile. The tropospheric NO_2 VCD simulated with the updated REAS emission inventory reasonably reproduced the NO_2 VCD from multisatellite observations, and its reproducibility was further improved by applying the AK to model results. However, additional research, including refining the updated REAS inventory in province-scale and comparative studies with other emission inventories, will be necessary to establish a more reliable inventory for East Asia. Our modeling results reproduced well the quantitative NO_2 VCD except during winter mornings, when the AK information applied to model results still tended to underestimate the observed NO_2 VCD. To clarify this issue, it will be necessary to consider modeling uncertainties, especially in relation to chemical reactions, in light of recent studies (Lin et al., 2012; Stavrakou et al., 2013). It will also be necessary to investigate uncertainties in satellite measurements through comparison with ground-based observations.

The differences between multisatellite observations and model sensitivity simulations in 2009 and 2010 with fixed emissions in 2008 implied an increase in NO_x emissions from 2008 levels. The model results and satellite observations of tropospheric NO_2 VCD were closely correlated with a linear relationship to anthropogenic NO_x emissions. Hence, a simple inverse estimate of NO_x emissions was proposed. On the basis of the NO_2 VCD observed by satellite, the anthropogenic NO_x emissions in 2009 and 2010 were estimated using linear regression results. Using this approach, we estimated anthropogenic NO_x emissions from China as $26.4\,\mathrm{Tg\,year}^{-1}$ in 2009 and $28.5\,\mathrm{Tg\,year}^{-1}$ in 2010, indicating that emissions more than doubled from 2000 to 2010. This means that there was a strong increase in anthropogenic emissions in China and rapid recovery of the Chinese economy from economic recession. Our estimates were consistent with the latest estimations of NO_x emissions in China.

Acknowledgements. This work was supported in part by the Global Environment Research Fund (S-7) of the Ministry of Environment, Japan. We are grateful for the use of the tropospheric NO_2 data set obtained from www.temis.nl. We thank K. Yumimoto of the Meteorological Research Institute for his comments on usage of satellite retrieval data sets. We also thank K. Yamaji and K. Ikeda of the Research Institute for Global Change, Japan Agency for Marine-Earth Science and Technology (JAMSTEC), for their comments on the CMAQ calculations.

Edited by: C. H. Song

References

Boersma, K. F., Eskes, H. J., and Brinksma, E. J.: Error analysis for tropospheric NO_2 retrieval from space, J. Geophys. Res., 109, D04311, doi:10.1029/2003JD003962, 2004.

Boersma, K. F., Eskes, H. J., Veefkind, J. P., Brinksma, E. J., van der A, R. J., Sneep, M., van den Oord, G. H. J., Levelt, P. F., Stammes, P., Gleason, J. F., and Bucsela, E. J.: Near-real time retrieval of tropospheric NO_2 from OMI, Atmos. Chem. Phys., 7, 2103–2118, doi:10.5194/acp-7-2103-2007, 2007.

Boersma, K. F., Eskes, H. J., Dirksen, R. J., van der A, R. J., Veefkind, J. P., Stammes, P., Huijnen, V., Kleipool, Q. L., Sneep, M., Claas, J., Leitão, J., Richter, A., Zhou, Y., and Brunner, D.: An improved tropospheric NO_2 column retrieval algorithm for the Ozone Monitoring Instrument, Atmos. Meas. Tech., 4, 1905–1928, doi:10.5194/amt-4-1905-2011, 2011.

Byun, D. W. and Ching, J. K. S.,: Science Algorithms of the EPA Model-3 Community Multiscale Air Quality (CMAQ) Modeling System, U.S. Environmental Protection Agency Rep. EPA-600/R-99/030, 727 pp., 1999.

Byun, D. W. and Schere, K. L.: Review of the governing equations, computational algorithms, and other components of the Model-3 Community Multiscale Air Quality (CMAQ) modeling system, Appl. Mech. Rev., 59, 51–77, 2006.

Carlton, A. G., Bhave, P. V., Napelenok, S. L., Edney, E. O., Sarwar, G., Pinder, R. W., Pouliot, G. A., and Houyoux, M.: Model representation of secondary organic aerosol in CMAQ v4.7, Environ. Sci. Technol., 44, 8553–8560, 2010.

Carter, W. P. L.: Documentation of the SAPRC-99 chemical mechanism for VOC reactivity assessment, Final report to California Air Resource Board, Sacramento, CA, 2000.

Guenther, A., Karl, T., Harley, P., Wiedinmyer, C., Palmer, P. I., and Geron, C.: Estimates of global terrestrial isoprene emissions using MEGAN (Model of Emissions of Gases and Aerosols from

Nature), Atmos. Chem. Phys., 6, 3181–3210, doi:10.5194/acp-6-3181-2006, 2006.

Han, K. M., Song, C. H., Ahn, H. J., Park, R. S., Woo, J. H., Lee, C. K., Richter, A., Burrows, J. P., Kim, J. Y., and Hong, J. H.: Investigation of NO_x emissions and NO_x-related chemistry in East Asia using CMAQ-predicted and GOME-derived NO_2 columns, Atmos. Chem. Phys., 9, 1017–1036, doi:10.5194/acp-9-1017-2009, 2009.

He, K.: Multi-resolution Emission Inventory for China (MEIC): Model framework and 1990–2010 anthropogenic emissions, International Global Atmospheric Chemistry Conference, Beijing, China, 2012.

He, Y.-J., Uno, I., Wang, Z., Ohara, T., Sugimoto. N., Shimizu, A., Richter, A., and Burrows, J. P.: Variations of the increasing trend of tropospheric NO_2 over east China during the past decade, Atmos. Environ., 41, 4865–4876, 2007.

Irie, H., Kanaya, Y., Takashima, H., Gleason, J. F., and Wang, Z.: Characterization of OMI tropospheric NO_2 measurements in East Asia based on a robust validation comparison, SOLA, 5, 117–120, doi:10.2151/sola.2009-030, 2009.

Irie, H., Boersma, K. F., Kanaya, Y., Takashima, H., Pan, X., and Wang, Z. F.: Quantitative bias estimates for tropospheric NO_2 columns retrieved from SCIAMACHY, OMI, and GOME-2 using a common standard for East Asia, Atmos. Meas. Tech., 5, 2403–2411, doi:10.5194/amt-5-2403-2012, 2012.

Irie, H., Yamaji, K., Ikeda, K., Uno, I., Itahashi, S., Ohara, T., and Kurokawa, J.: An evaluation of the CMAQ reproducibility of satellite tropospheric NO_2 column observations at different local times over East Asia, Atmos. Chem. Phys. Discuss., 13, 14037–14067, doi:10.5194/acpd-13-14037-2013, 2013.

Itahashi, S., Uno, I., Yumimoto, K., Irie, H., Osada, K., Ogata, K., Fukushima, H., Wang, Z., and Ohara, T.: Interannual variation in the fine-mode MODIS aerosol optical depth and its relationship to the changes in sulfur dioxide emissions in China between 2000 and 2010, Atmos. Chem. Phys., 12, 2631–2640, doi:10.5194/acp-12-2631-2012, 2012a.

Itahashi, S., Uno, I., and Kim, S-T.: Source contributions of sulfate aerosol over East Asia estimated by CMAQ-DDM, Environ. Sci. Technol., 46, 6733–6741, 2012b.

Itahashi, S., Uno, I., and Kim, S-T.: Seasonal source contributions of tropospheric ozone over East Asia based on CMAQ-HDDM, Atmos. Environ., 70, 204–217, 2013.

Kurokawa, J., K. Yumimoto, Uno, I., and Ohara, T.: Adjoint inverse modeling of NO_x emissions over eastern China using satellite observations of NO_2 vertical column densities, Atmos. Environ., 43, 1878–1887, 2009.

Kurokawa, J., Ohara, T., Morikawa, T., Hanayama, S., Janssens-Maenhout, G., Fukui, T., Kawashima, K., and Akimoto, H.: Emissions of air pollutants and greenhouse gases over Asian regions during 2000–2008: Regional Emission inventory in ASia (REAS) version 2, Atmos. Chem. Phys., 13, 11019–11058, doi:10.5194/acp-13-11019-2013, 2013.

Lamsal, L. N., Martin, R. V., Padmanabhan, A., van Donkelaar, A, Zhang, Q., Sioris, C. E., Chance, K., Kurosu, T. P., and Newchurch, M. J.: Application of satellite observations for timely updates to global anthropogenic NO_x emission inventory, Geophys. Res. Lett., 38, L05810, doi:10.1029/2010GL046476, 2011.

Lin, J.-T. and McElroy, M. B.: Detection from space of a reduction in anthropogenic emissions of nitrogen oxides during the Chinese economic downturn, Atmos. Chem. Phys., 11, 8171–8188, doi:10.5194/acp-11-8171-2011, 2011.

Lin, J.-T.: Satellite constraint for emissions of nitrogen oxides from anthropogenic, lightning and soil sources over East China on a high-resolution grid, Atmos. Chem. Phys., 12, 2881–2898, doi:10.5194/acp-12-2881-2012, 2012.

Lin, J.-T., Liu, Z., Zhang, Q., Liu, H., Mao, J., and Zhuang, G.: Modeling uncertainties for tropospheric nitrogen dioxide columns affecting satellite-based inverse modeling of nitrogen oxides emissions, Atmos. Chem. Phys., 12, 12255–12275, doi:10.5194/acp-12-12255-2012, 2012.

Lu, Z., Streets, D. G., Zhang, Q., Wang, S., Carmichael, G. R., Cheng, Y. F., Wei, C., Chin, M., Diehl, T., and Tan, Q.: Sulfur dioxide emissions in China and sulfur trends in East Asia since 2000, Atmos. Chem. Phys., 10, 6311–6331, doi:10.5194/acp-10-6311-2010, 2010.

Martin, R. V., Jacob, D. J., Chance, K., Kurosu, T. P, Palmer, P. I., and Evans, M. J.: Global inventory of nitrogen oxide emissions constrained by space-based observations of NO_2 columns, J. Geophys. Res., 108, 4537, doi:10.1029/2003JD003453, 2003.

Odman, M. T. and Russell, A. G.: Mass conservative coupling of non-hydrostatic meteorological models with air quality models. Air Pollution Modeling and Its Application XIII, Kluwer Academic/Plenum Publishers, New York, 651–660, 2000.

Ohara, T., Akimoto, H., Kurokawa, J., Horii, N., Yamaji, K., Yan, X., and Hayasaka, T.: An Asian emission inventory of anthropogenic emission sources for the period 1980–2020, Atmos. Chem. Phys., 7, 4419–4444, doi:10.5194/acp-7-4419-2007, 2007.

Richter, A., Burrows, J. P., Nues, H., Granier, C., and Niemeier, U.: Increase in tropospheric nitrogen dioxide over China observed from space, Nature, 437, 129–132, 2005.

Schneider, P. and van der A, R. J.: A global single-sensor analysis of 2002–2011 tropospheric nitrogen dioxide trends observed from space, J. Geophys. Res., 117, D16309, doi:10.1029/2012JD017571, 2012.

Seinfeld, J. H. and Pandis, S. N.: Atmospheric Chemistry and Physics: From Air Pollution to Climate Change, Second Edn., John Wiley & Sons, Inc., Hoboken, New Jersey, USA, 2006.

Stavrakou, T., Müller, J.-F., Boersma, K. F., van der A, R. J., Kurokawa, J., Ohara, T., and Zhang, Q.: Key chemical NO_x sink uncertainties and how they influence top-down emissions of nitrogen oxides, Atmos. Chem. Phys., 13, 9057–9082, doi:10.5194/acp-13-9057-2013, 2013.

Sudo, K., Takahashi, M., Kurokawa, J., and Akimoto, H.: CHASER: a global chemical model of the troposphere 1. Model description, J. Geophys. Res., 107, 4339, doi:10.1029/2001JD001113 , 2002.

Uno, I., He, Y., Ohara, T., Yamaji, K., Kurokawa, J.-I., Katayama, M., Wang, Z., Noguchi, K., Hayashida, S., Richter, A., and Burrows, J. P.: Systematic analysis of interannual and seasonal variations of model-simulated tropospheric NO_2 in Asia and comparison with GOME-satellite data, Atmos. Chem. Phys., 7, 1671–1681, doi:10.5194/acp-7-1671-2007, 2007.

van der A, R. J., Eskes, H. J., Boersma, K. F., van Noije, T. P. C., Van Roozendael, M., De Smedt, I., Peters, D. H. M. U., and Meijer, E. W.: Trends, seasonal variability and dominant NO_x source derived from a ten year record of NO_2 measured from space, J. Geophys. Res., 113, D04302, doi:10.1029/2007JD009021, 2008.

van der Werf, G. R., Randerson, J. T., Giglio, L., Collatz, G. J., Mu, M., Kasibhatla, P. S., Morton, D. C., DeFries, R. S., Jin, Y., and van Leeuwen, T. T.: Global fire emissions and the contribution of deforestation, savanna, forest, agricultural, and peat fires (1997–2009), Atmos. Chem. Phys., 10, 11707–11735, doi:10.5194/acp-10-11707-2010, 2010.

Zhao, B., Wang, S. X., Liu, H., Xu, J. Y., Fu, K., Klimont, Z., Hao, J. M., He, K. B., Cofala, J., and Amann, M.: NO_x emissions in China: historical trends and future perspectives, Atmos. Chem. Phys., 13, 9869–9897, doi:10.5194/acp-13-9869-2013, 2013.

Zhao, Y., Zhang, J., and Nielsen, C. P.: The effects of recent control policies on trends in emissions of anthropogenic atmospheric pollutants and CO2 in China, Atmos. Chem. Phys., 13, 487–508, doi:10.5194/acp-13-487-2013, 2013.